Advances in Science and Technology Research Journal

Advances in Science and Technology Research Journal 2023, 17(2), 247–257
https://doi.org/10.12913/22998624/161690
ISSN 2299–8624, License CC-BY 4.0

Received: 2023.02.07
Accepted: 2023.03.15
Published: 2023.04.01

Effect of Volume Percentage of Reinforcement on the Microstructure and Mechanical Properties of an Al6061-T6/SiC Surface Composite Fabricated Through Friction Stir Processing

Abdul Jabbar Ansari[1*], Mohd. Anas[1]

[1] Department of Mechanical Engineering, Integral University, Kursi Road, Lucknow, 226026, India
* Corresponding author email: techno.abdul@gmail.com

ABSTRACT

In this research, aluminium metal matrix composites (AMMCs) have been manufactured through friction stir processing (FSP) by reinforcing micro sized SiC particles in an Al6061-T6 alloy. The consequences of the volume percentage of reinforced SiC particles on mechanical properties and microstructural features were analyzed for the developed AMMCs. Microstructural evaluation of a cross-section of a friction stir processed (FSPed) sample has been conducted through Electron backscatter diffraction (EBSD) Energy dispersive spectroscopy (EDS) and a scanning electron microscope (SEM) technique. Microhardness tests were conducted athwart the cross section of FSPed specimen to obtain microhardness feature. A tensile test of FSPed samples has been conducted on a universal testing machine (UTM). Homogeneous distributions of SiC particles were found in the stir zone without any consolidation of particles. The size of the reinforcement particles was decreased slightly by increasing the volume fraction. It has been found that increasing the volume fraction of SiC particles, enhance the tensile strength and microhardness, but decreases the ductility of the aluminium. The maximum ultimate tensile strength (UTS) and microhardness were obtained as 390 MPa and 150.71 HV, respectively, at 12% volume percentage of reinforcement particles. UTS and microhardness of the FSPed Al/SiC have been improved by 38.29% and 59.48% respectively as compared to Al6061-T6. The brittle nature of the FSPed Al/SiC has increased due to a rise in the volume fraction of micro sized SiC particles, which causes a decrease in ductility.

Keywords: friction stir processing, aluminium metal matrix composite, silicon carbide, microstructure, surface composite, composite material.

INTRODUCTION

In FSP, due to the rotational and translational motion of the tool, microstructure and mechanical behaviour of the metal can be altered [1, 2]. Visco plastic movement of material started due to the stirring operation of the tool. The FSP tool started moving in the processing direction at traverse speed. Softening of the base metal started due to the heat generated between the FSP tool and base metal. Many researchers have fabricated surface composites using nanosize reinforcement particles [3, 4]. Some researchers investigated the effect and feasibility of an aluminium alloy by reinforcing different nanoparticles [5–7]. In the structural application of the automobile and aerospace industries, the FSW/FSP technique is widely used. In 1998, NASA implemented this technique to fabricate the external tank of the space shuttle [8]. The U.S. Navy used the FSW technique to fabricate AA5083 and AA6061 aluminium alloys [8]. The major utilization of the FSP is the alteration in the mechanical behaviour and refinement of the microstructure of the metallic surface [9]. An effective and proper treatment to obtain refined microstructure, results in homogeneity of the base metal's processed zone [10]. The hardness property of the composites Al/Gr and Al/MOS_2 manufactured through FSP were increased by and 75.26% and 55.6%, respectively, in comparison to base metal, while the wear resistance properties of Al/Gr and Al/MOS_2 were

decreased by 24.35% and 33.5%, respectively, in comparison to the base metal [11]. The variation in wear resistance and hardness of the composite AA1120 with feed rate was observed. It increased up to 56 mm/min, and after that, the wear rate enhanced while the hardness of the composite reduced [12]. In the fabrication of AMMCs with hybrid micro and nano-reinforcement, the FSP technique has better potential due to its high temperature and severe plastic deformation and mixing as compared to other fabrication processes [13, 14]. The FSP technique produces excellent results with reinforcement of different hybrid nanoparticles [15, 16].

Type of reinforcement and processing parameters of FSP mostly influence the mechanical behaviour of the surface composite. Threaded pin profile of the FSP tool produced uniform distribution of reinforcement particles [17, 18]. The microhardness of the surface composite 5A06Al/SiC was enhanced by 10% through the FSP technique [19]. In the composite fabrication of AA1050/SiC through FSP, the microhardness was increased by 139% [20]. Increment in wear resistance and microhardness of the surface composite AA5083/SiC fabricated using the FSP technique were observed by 48% and 51%, respectively [21]. Many researchers obtained good results by incorporating nanoparticles like graphite, Cu, and ceramic B_4C in AMMCs through the FSP technique [22–24].

Electron beam radiation, powder metallurgy, stir casting and hot pressing are commonly applicable techniques for the fabrication of the composite. At high temperature in the liquid phase, unwanted substrate developed in the composite. Agglomeration of the reinforcement was observed in the composite due to high density difference and uneven distribution of reinforcement [25, 26]. Some common defects like brittle intermetallic formation, agglomeration and high manufacturing cost were generally observed in these conventional methods. The FSP technique is an exceptional manufacturing technique because surface properties of the base metal are altered while inherent properties remain same. FSP is basically used to revise the granular structure, to refined microstructure, lower defects and dissolve secondary particles which observed during the conventional processes [27].

Reinforcement of SiC particles does not create any undesirable phases in the composite [28, 29]. Limited research is available on the varying volume fraction of reinforced particles in Al6061-T6/SiC composites through FSP. In this experimental work, FSP method has been applied for modification of the mechanical properties of Al6061-T6. Microstructure and mechanical behaviour of Al6061-T6/SiC AMMCs have been investigated by changing the volume percentage of micro size SiC particles.

EXPERIMENTAL PROCEDURE

Aluminium alloy Al6061-T6 of dimension 250 mm × 75 mm × 6 mm were selected as base metal. The composition of the base metal is shown in Table 1. Some basic mechanical properties of base metal are listed in Table 2. All data of chemical composition has been obtained by spectro test and properties of base metal have been taken as per ASM material data sheet.

At the centre line of the base plate, a square groove was machined using milling cutter. Three different groove dimensions for an 8%, 10%, and 12% volume fraction are created at base metal. The variation in groove size is calculated based on three levels of fractional volume of reinforcement particle (8%, 10%, and 12%) in the processed region of SCs. The groove dimensions on the basis of the selected volume fraction were calculated using Equations 1 and 2 [39].

$$Fractional\ volume\ \% = \\ = \frac{Area\ of\ groove}{Projected\ area\ of\ SZ} \times 100 \tag{1}$$

$$Area\ of\ groove = \\ = Groove\ width \times Groove\ depth \tag{2}$$

From the previous studies it is observed that in FSP, flow of material due to the motion of tool follows two mechanisms, one is "material flow by shoulder of tool" and second is "flow of material by tool pin" [30]. Due to these two mechanisms, width of the stir zone steadily decreases from top to bottom. Hence for more precise dimensions, the projected area of the stir zone is assumed to be a half parabola. The projected area of the stir

zone is calculated by the integration method to find out the area bounded by the curve with the help of Equation 3.

$$projected\ area\ of\ SZ\ (area\ of\ parabola)\ A = \frac{2ab}{3} \quad (3)$$

where: a – tool shoulder diameter
b – l + y,
l – tool pin lenght
y – height of isosceles triangle
d – tool pin diameter

Height of isosceles triangle calculated as

$$y = \frac{d}{2} \tan 15 \quad (4)$$

After machining a groove on the Al6061-T6 base metal, the plates were cleaned using acetone to remove dust particles. Micro size SiC particles with 99% purity were selected as reinforcement. Magnified SEM image of the micro size reinforcement SiC particles are shown in Figure 1a. The reinforcement particles were properly filled in the groove. A pinless tool of shoulder diameter 20 mm was used to cover the reinforcement particles sputtering out of the groove. After using pinless tool, a threaded pin profile built of H13 tool steel with 6 mm diameter and 4 mm length was selected for FSP. Tool shoulder diameter was taken at 20 mm, as shown in Figure 1b. On the basis of literature survey it is found that apart from these important parameters such as tool shoulder diameter, tool rotational speed, and tool traverse speed, there are many other parameters such as tool tilt angle, tool plunge depth, axial load, dwell time etc. affect the quality of surface composite. Many trial experiments were performed for selecting the process parameters for the fabrication of surface composite on Al6061-T6. The performance of FSP was evaluated on the basis of processed surface of plate without defects, processed zone, machine without vibration and noise during processing. Different processing parameters of FSP used in this experiment are listed in Table 3.

First, FSP was carried out without any reinforcement in the base metal. Then FSP was carried out on different volume fraction of reinforced SiC particles. Three varying volume fractions (8%, 10%, and 12%) of reinforcement were selected on fixed levels of process parameters and dimension of tool to obtain the exclusive effect of different volume percentage of micro size SiC on the mechanical behaviour and microstructure of AMMCs. All defect free samples prepared through the FSP technique are shown in Figure 2.

Specimens for microstructural observation were prepared from the stir zone of the sample. According to standard procedure, all specimens were polished using grinding papers of various grit sizes (120, 220, 320, 400, 600, 800, and 1000). After that, the samples were polished by diamond polishing. EBSD and SEM technique is used for the characterization of prepared samples using a Zeiss Gemini SEM 300. Microhardness test sample prepared according to ASTM E384 standard. Microhardness tests of the samples were carried out using a 500 gram load for around 10 seconds. The microhardness test was accomplished on the samples in cross section at a point located 2 mm beneath the upper surface along a 0.5 mm horizontally spaced line using a Vickers hardness machine. The final microhardness value was taken as the average of the three measured values.. Tensile test specimen prepared from the FSPed sample using wire EDM. Specimen is removed from stir zone in which tensile axis was seized as alongside to the direction of FSP and prepared according to ASTM D638 standard.

RESULTS AND DISCUSSION

Microstructure of Al6061-T6/SiC AMMCs

The SEM micrographs of the fabricated Al6061-T6/SiC composites are shown in Figure 3a–c and the composition in EDS map at 12% SiC volume fraction shown in Figure 4. It can be revealed that the reinforced SiC in AMMCs are uniformly distributed. Material moves from advancing side to retreating side due to the rotational motion of tool. The plasticized material

Table 1. Elemental composition of Al6061-T6 (obtained by spectro test)

Mg	Si	Cu	Fe	Mn	Cr	Al
0.895%	0.623%	0.297%	0.279%	0.414%	0.214%	Remainder

Table 2 Properties of Al6061-T6

S.N.	Properties	Value
1	Ultimate tensile strength	310 (MPa)
2	Young's modulus	68.9 GPa
3	Possion's ratio	0.33
4	Elongation at break	12%
5	Density	2.70 g/cm^3

is assembled at rear of the tool. The plasticized aluminium material was combined and mixed with reinforced SiC particles because rotational motion of tool creates stirring effect. Clustering and accumulation of the reinforcement are mostly as a result of density gradient. The whole process of FSP is completed in a solid state of metal without melting the aluminium matrix. Hence, no free flow of the particles occurred due to the difference in density in FSP. The bonding between the aluminium and SiC perform a major role in transferring the load during tensile loading. Enhanced mechanical properties are obtained at high interfacial bonding between aluminium and SiC particles. The high temperature during AMMCs formation has a significant impact on interfacial bonding. When the formation of AMMCs takes place at higher temperature, intermetallic is formed. This intermetallic weakens the bonding between aluminium and SiC particles. The temperature required to initiate an interfacial reaction is not produced during the FSP. Hence, no such intermetallic is formed during FSP [31].

On the basis of the quantitative analysis of SEM images displayed in Figure 3, it is revealed that the size of the reinforcement is slightly refined. The reason behind the refinement of the reinforced particle's size is the tool's rotational motion and the high plastic strain. This joint action reduces the SiC particle size. By enhancing the volume percentage of reinforcement from 8 to 12 percent, the intermediate size of the reinforcement has been reduced. This action was possible may be due to two factors. Firstly, flow stress is improved as a result of enhancement in the volume percentage of reinforcement because SiC particles have high non-deformability. Second, due to their heat sinking property, SiC particles absorb heat generated due to the friction available between base metal and FSP tool. Hence, by enhancing the volume percentage of the reinforced SiC particles, the temperature of stir zone reduced, which resulted in an increase in flow stress. Figure 5 shows the EBSD images of Al6061-T6, FSPed Al6061-T6 and AMMCs. It can be observed that coarse and elongated grains in base metal were replaced by refined grains in AMMCs. The average grain size in AMMCs was decreased due to the dynamic recrystallization. Similar results were obtained by Huang G. et al [36].

Microhardness

Heat available by the relative motion between base metal and tool, initiates the dynamic recrystallization of grains and may cause the development of strain-free grains. The average microhardness value of each sample is listed in Table 4. The microhardness profile all samples are displayed in Figure 6. It can be seen that by increasing the volume percentage of reinforcement, the average microhardness of the sample increased. A maximum microhardness value of 150.71 HV is obtained at a 12% of SiC particles in AMMCs. When a load is acted to the FSPed composite, the load is transferred from the matrix to the reinforced material,

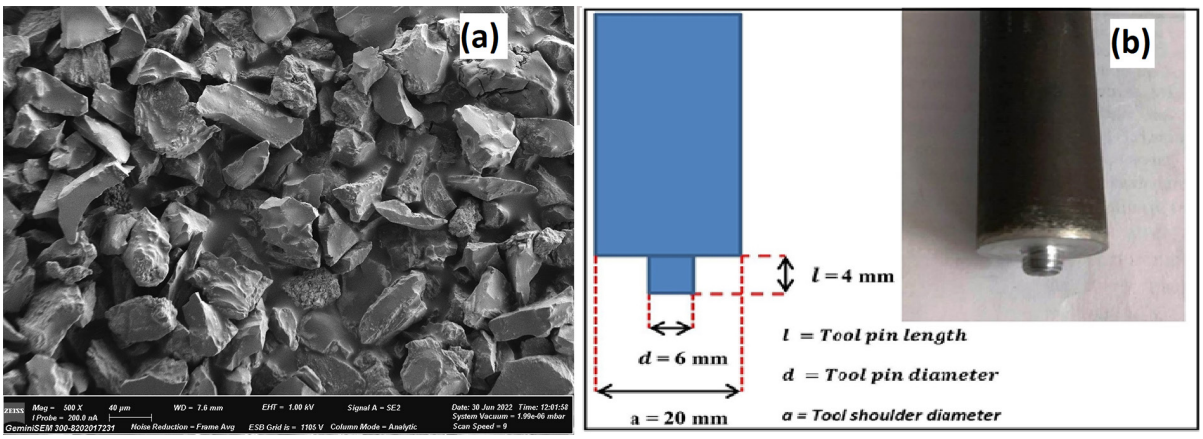

Figure 1. SEM image of micro size SiC particles (a), Dimension of tool used in FSP (b)

Table 3. Value of FSP parameters

S.N.	Fixed Parameters	Value
1	Rotational speed of tool (rpm)	800
2	Traverse speed of tool (mm/min)	50
3	Tilt angle of tool (degrees)	2°
4	Plunge depth of tool (mm)	0.2
5	Dwell time (second)	15
6	Axial load (kN)	100

resulting in increased AMMCs strength [32]. Due to plasticized matrix deformation, large density dislocations were formed, resulting in increased composite strength [33, 34]. SiC particles have an extremely high hardness, which increases the hardness of the composite through their uniform distribution. According to the Hall-Patch equation, more grain boundaries are generated due to the refinement of grains, which results in more difficulties in dislocation slip. Greater stress is needed for plastic deformation of the material. Because interparticle spacing decreases with increasing SiC particle concentration, it is possible that during hardness testing, the indentator will strike on the SiC particles, increasing the composite's microhardness value [35].

Tensile properties

The stress strain curve and main tensile properties of all samples are presented in Figures 7 and 8, respectively. The tensile strength profile depicts that the UTS improves with the enhancement in the volume percentage of SiC particles. Identical results were obtained by Haung et. al [36]. Grain size refinement is observed in the FSPed sample, which enhances the tensile strength of the sample according to the Hall-Patch grain refinement strengthening equation [35]. The pinning effect of increasing reinforcement particle homogeneity in AMMCs inhibits dislocation movement, and thus necessary stress (Orowan strengthening) is evaluated for overcoming dislocation movement [37]. The interparticle space between reinforced SiC particles decreases due to the enhancement in the volume percentage of the reinforcement,

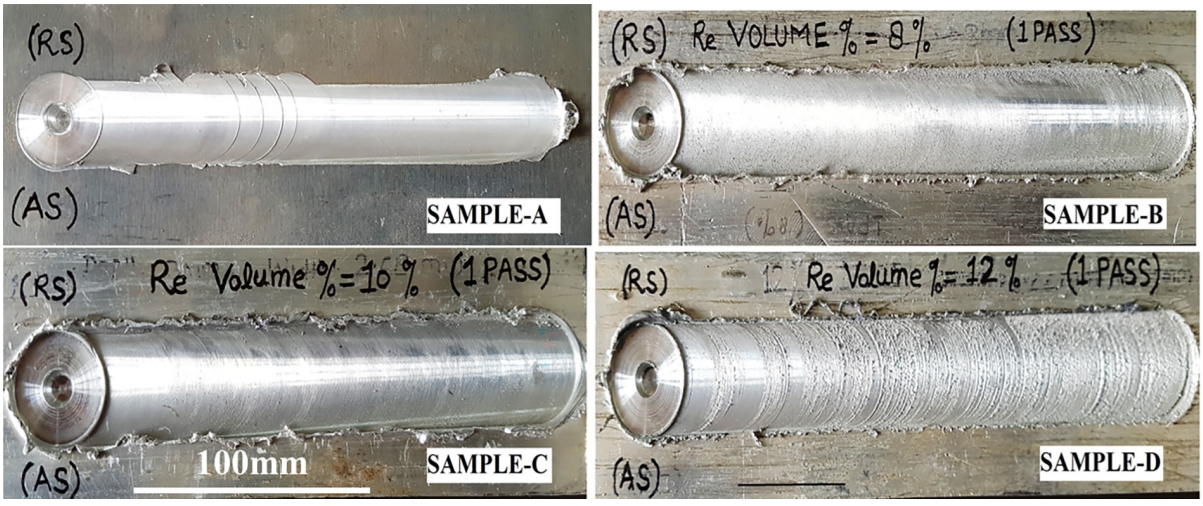

Figure 2. Defect free samples fabricated through FSP technique (a) FSPed base Al6061-T6, (b) Al6061-T6/SiC 8% volume fraction, (c) Al6061-T6/SiC 10%, (d) Al6061-T6/SiC 12%

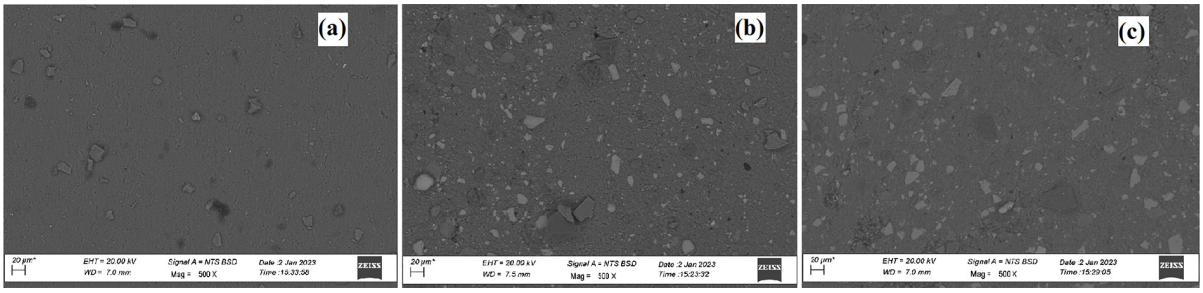

Figure 3. SEM micrograph of the FSPed sample (a) Al6061/SiC 8% volume fraction, (b) Al6061/SiC 10% volume fraction, (c) Al6061/SiC 12% volume fraction

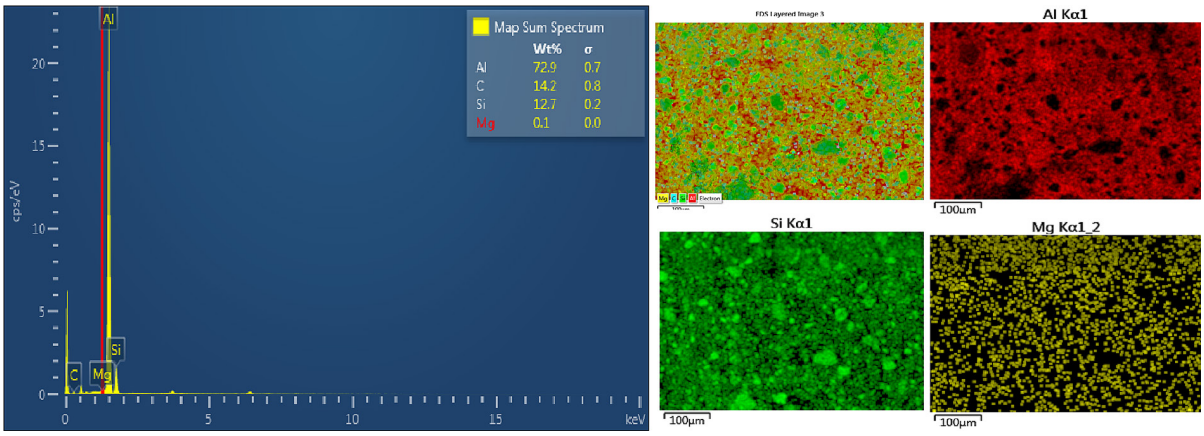

Figure 4. Distribution and composition of Al, Si and Mg elements

which results in enhanced strength and bonding in the matrix. As a result, AMMCs with 12% of reinforced particles has the highest UTS with a uniform dispersion of reinforced particles. The SEM picture of Al6061/SiC composite of 12% volume fraction displayed in Figure 3c clearly shows a uniform distribution of SiC materials. Size of the particles is decreased due to the high amount of strain produced at the optimum volume percentage of SiC particles and the tool's stirring action. Maximum yield strength (YS) of 290 MPa and UTS of 390 MPa were obtained at 12% volume fraction. The UTS and YS were enhanced by 38.29% and 48.71%, respectively, in comparison of Al6061-T6 alloy. Apart from this, the ductility of the unreinforced FSPed Al 6061-T6 was increased as compared to the base metal Al6061-T6. Work hardening capability is improved by the development of fine grains with depressed dislocation density [38, 39]. However, the ductility of FSPed Al6061-T6 has decreased with the increase in SiC particles. As we know, the microvoids are created at the site of dislocation accumulation. During tensile deformation, cracks are initiated at these fragile parts adjacent to the Al/SiC interface. Despite better interfacial

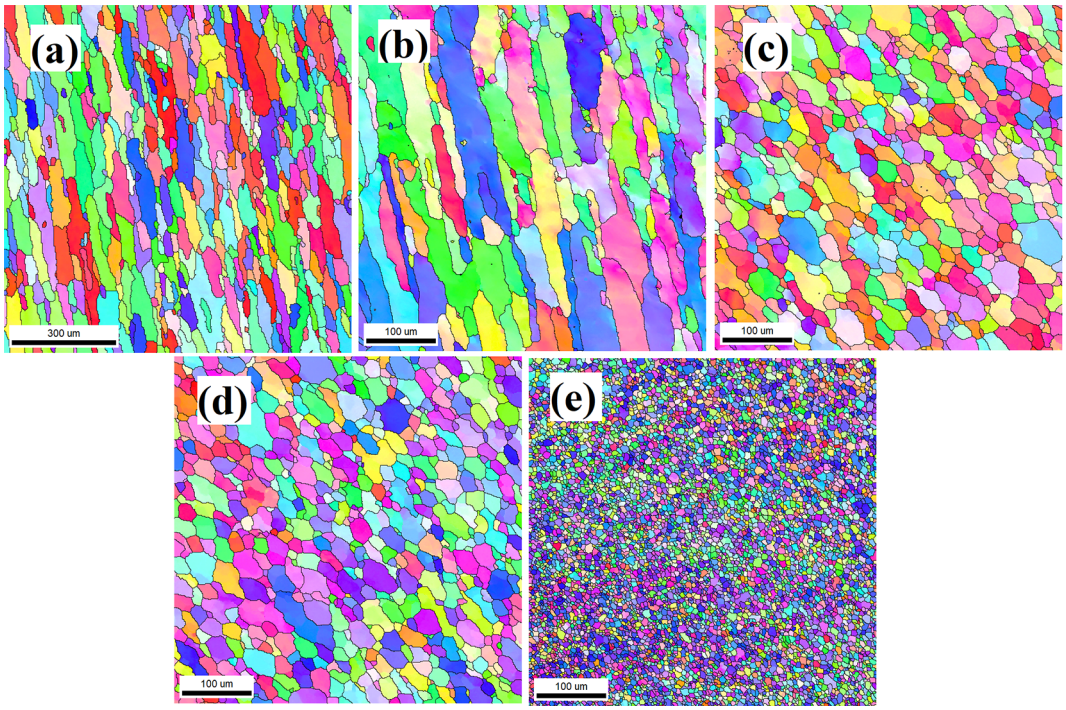

Figure 5. EBSD image of (a) Al6061-T6, (b) FSPed Al6061-T6, (c) Al6061/SiC 8% volume fraction, (d) Al6061/SiC 10% volume fraction, (e) Al6061/SiC 12% volume fraction

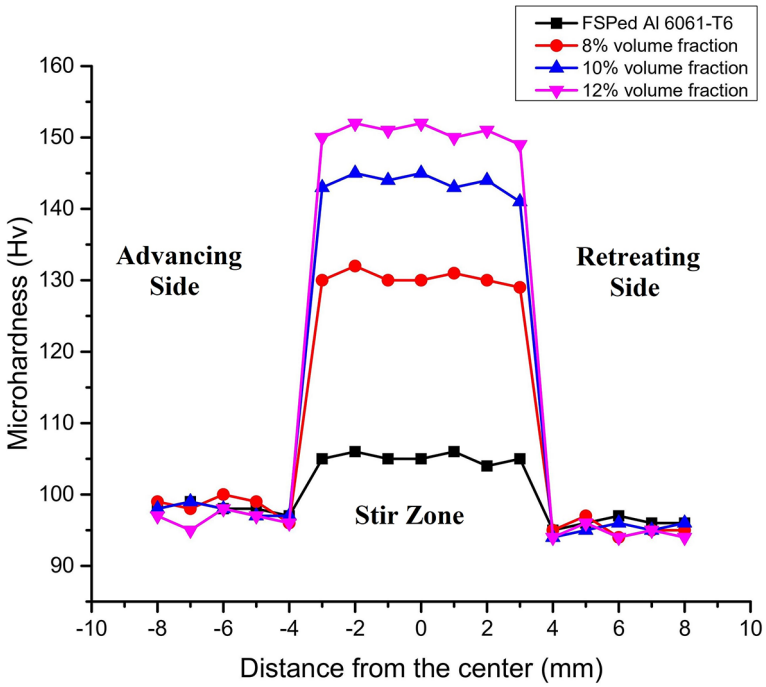

Figure 6. Microhardness distribution of the FSPed composite

Table 4. List of results obtained after testing of samples

S.N.	Sample	Average Hardness (HV4.9)	UTS (MPa)	YS (MPa)	Percentage elongation
1	As received Al6061-T6	94.5	282	195	10
2	FSPed Al6061-T6	105.14	312	212	12
3	FSPed Al6061-T6/SiC 8% volume fraction	130.28	352	246	10.5
4	FSPed Al6061-T6/SiC 10% volume fraction	143.57	376	276	9.2
5	FSPed Al6061-T6/SiC 12% volume fraction	150.71	390	290	8.6

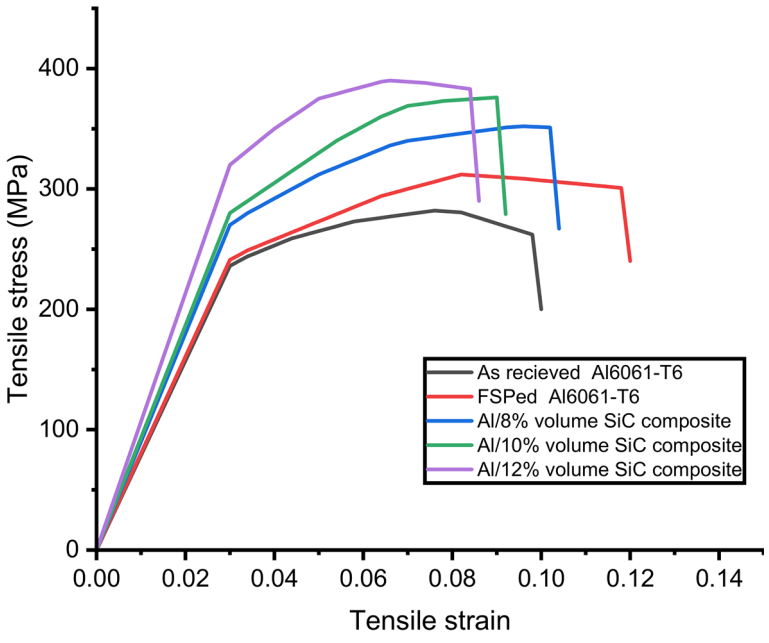

Figure 7. Stress-strain curve of Al6061-T6, FSPed Al and FSPed AMMCs

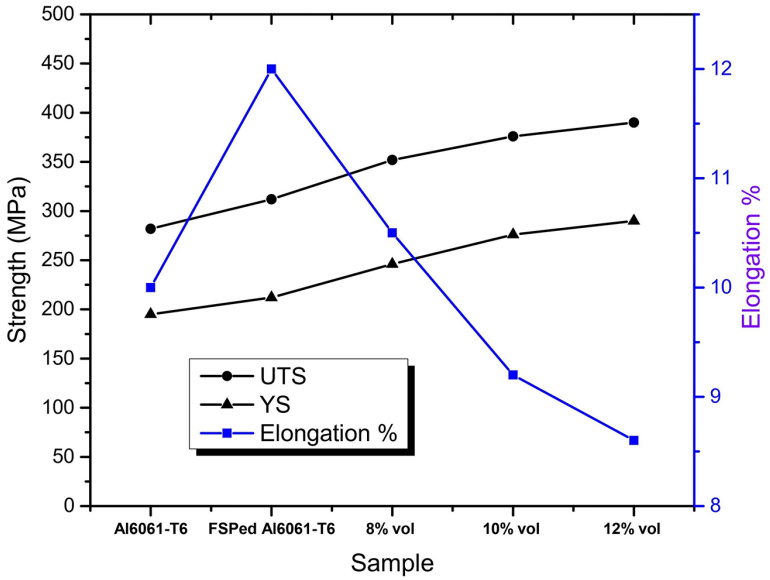

Figure 8. Variation in YS, UTS and percentage elongation of all samples.

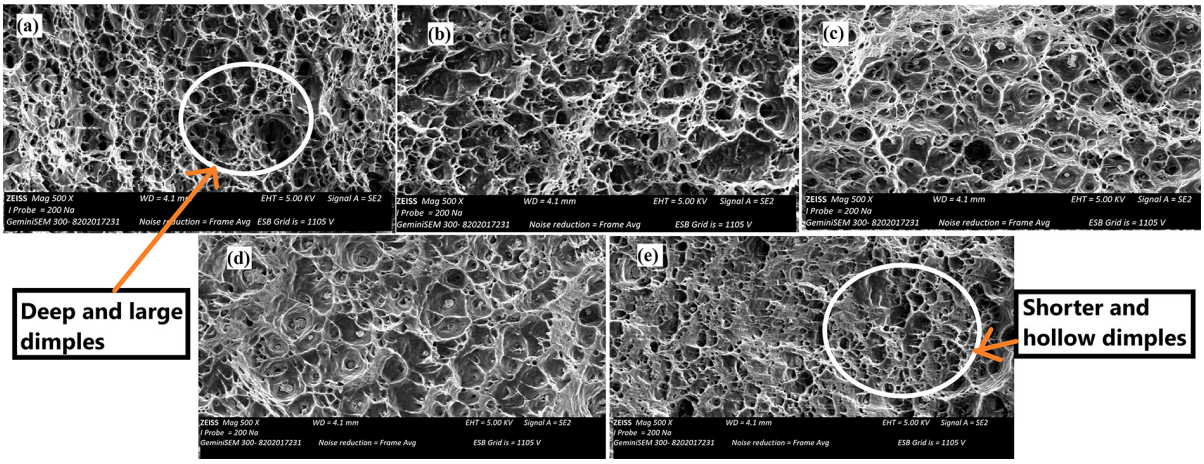

Figure 9. Tensile fractograph of (a) Al6061-T6, (b) FSPed Al 6061-T6, (c) AMMCs 8% volume fraction, (d) AMMCs 10% volume fraction, (e) AMMCs 12% volume fraction

bonding was observed in AMMCs, the weak areas in the AMMCs were increased by increasing the SiC particle volume fraction, which results in a reduction in ductility.

Fractography

The SEM pictures of the ruptured part of the sample after the tensile test are shown in Figure 9. Deep and large dimples, indicating typical ductile failure are shown in Figure 9a of the base metal. Slightly larger and deeper dimples are observed in the fractured surface of FSPed Al in Figure 9b, which is a good agreement in tensile testing. FSPed Al6061-T6 shows the highest elongation before fracture. When compared to Al6061-T6 and FSPed Al6061-T6, AMMCs have a greater number of shorter and hollow dimples shown in Figure 9c-e. The flatness of the surface of AMMCs enhances with the increase of SiC particle, attributing a reduction in AMMCs plastic deformation. It may be associated with their superior strength and hardness properties. Its capability for plastic deformation decreases with increase in flatness. In the observation of small dimples of AMMCs, large number of SiC particles has found which indicates that the bonding between the matrix and reinforced particles is robust. Hence no interfacial reaction processed in the AMMCs, which would reduce bonding

strength. However, further feeble regions of the Al/SiC interface were created by enhancing the volume percentage of reinforced SiC particles in AMMCs. Because of these weak regions, cracks initiate and propagate near the Al/SiC interface, resulting in early failure of AMMCs. Hence, the type of fracture becomes brittle, and ductility outset lowering with an increasing volume fraction of SiC particles in AMMCs.

CONCLUSIONS

In this experiment, Al6061-T6/SiC composites were fabricated through FSP technique with increasing volume percentage of reinforcement particles. Mechanical behaviour and microstructure of the prepared AMMCs were analyzed and obtained the consequences in the variation of volume fraction of reinforced SiC particles. The outcomes were concise below. Uniform and homogeneous dispersion of the SiC particles has been observed in AMMCs in different volume percentage of SiC particles. SiC particles were fragmented due to the rotational motion of tool and high plastic strain, which results in a decrease in size of reinforcement particles by enhancing volume percentage reinforcement particles. Defect free bonding between reinforcement and aluminium matrix was well established.

The high hindering consequence produced by reinforcement has reduced the size of grains, which accelerates the dynamic recrystallization of grains. The maximum microhardness, UTS, and YS of the composite were obtained as 150.71 HV, 390 MPa and 290 MPa, respectively, at 12% volume percentage of SiC particles in the AMMCs. Microhardness, UTS and YS of the AMMCs were improved by enhancing the volume fraction of SiC particles by 59.48%, 38.29% and 48.71% respectively. First, the ductility of FSPed Al6061-T6 increased, but after reinforcement with SiC particles, its ductility decreased. Also, the morphology of the fracture surface has changed.

Acknowledgments

The authors gratefully accede the mechanical engineering department and faculty of doctoral studies and research, Integral University, Lucknow (IU/R&D/2023-MCN0001879) for their technical support to perform this work.

REFERENCES

1. Rahmatian, Behrooz, Kamran Dehghani, and Seyyed Ehsan Mirsalehi. “Effect of adding SiC nanoparticles to nugget zone of thick AA5083 aluminium alloy joined by using double-sided friction stir welding.” Journal of Manufacturing Processes 2020; (52): 152–164.
2. Khodabakhshi F., Marzbanrad B., Shah L.H., Jahed H., Gerlich A.P. Friction-stir processing of a cold sprayed AA7075 coating layer on the AZ31B substrate: structural homogeneity, microstructures and hardness. Surface and Coatings Technology. 2017; 331: 116–128.
3. Patel, Sachin, Prateek Gupta, and Shyam Lal Verma. Optimization of hybrid composites 7075 Al fabricated by friction stir processing using Taguchi’s philosophy. Materials Today: Proceedings. 2022; 50: 2328–2335
4. Ansari, A.J., Anas, M. Review and analysis of the effect of variables on aluminium based surface composite fabricated through friction stir processing method. International Journal of Advanced Technology and Engineering Exploration. 2022; 9(95): 1552–1570.
5. Patel, Surendra Kumar, et al. Recent research progresses in Al-7075 based in-situ surface composite fabrication through friction stir processing: A review. Materials Science and Engineering: B. 2020; 262: 114708.
6. Tekiyeh, Ramin Mehdizad, Mohsen Najafi, and Saeid Shahraki. Machinability of AA7075-T6/carbon nanotube surface composite fabricated by friction stir processing. Proceedings of the Institution of Mechanical Engineers, Part E: Journal of Process Mechanical Engineering. 2019; 233(4): 839–848.
7. Uzun H. Friction stir welding of SiC particulate reinforced AA2124 aluminium alloy matrix composite. Materials & design. 2007; 28(5): 1440–1446.
8. Gibson B.T., Lammlein D.H., Prater T.J., Longhurst W.R., Cox C.D., Ballun M.C., Dharmaraj K.J., Cook G.E., Strauss A.M. Friction stir welding: Process, automation, and control. Journal of Manufacturing Processes. 2014; 16(1): 56–73.
9. Deepati A.K., Alhazmi W., Zakri W., Shaban E., Biswas P. Parametric Analysis on the Progression of Mechanical Properties on FSW of Aluminum-Copper Plates. Advances in Science and Technology Research Journal. 2022; 16(2): 168–178. https://doi.org/10.12913/22998624/147123
10. Chang C.I., Du X.H., Huang J.C. Achieving ultrafine grain size in Mg–Al–Zn alloy by friction stir processing. Scripta Materialia. 2007; 57(3): 209–212.

11. Gupta M.K. Analysis of tribological behavior of Al/Gr/MoS2 surface composite fabricated by friction stir process. Carbon letters. 2020; 30(4): 399–408.
12. Gupta M.K. Effects of tool pin profile and feed rate on wear performance of pine leaf ash/Al composite prepared by friction stir processing. Journal of Adhesion Science and Technology. 2021; 35(3): 256–268.
13. Khodabakhshi F., Gerlich A.P., Simchi A., Kokabi A.H. Hot deformation behavior of an aluminum-matrix hybrid nanocomposite fabricated by friction stir processing. Materials Science and Engineering: A. 2015; 626: 458–466.
14. Soleymani S., Abdollah-Zadeh A., Alidokht S.A. Microstructural and tribological properties of Al5083 based surface hybrid composite produced by friction stir processing. Wear. 2012; 278: 41–47.
15. Adel Mehraban F., Karimzadeh F., Abbasi M.H. Development of surface nanocomposite based on Al-Ni-O ternary system on Al6061 alloy by friction-stir processing and evaluation of its properties. JOM. 2015; 67: 998–1006.
16. Asl A.M., Khandani S.T. Role of hybrid ratio in microstructural, mechanical and sliding wear properties of the Al5083/Graphitep/Al2O3p a surface hybrid nanocomposite fabricated via friction stir processing method. Materials Science and Engineering: A. 2013; 559: 549–557.
17. Gupta M.K. Friction stir process: a green fabrication technique for surface composites–a review paper. SN Applied Sciences. 2020: 1–4.
18. Gupta M.K. Effects of tool profile on mechanical properties of aluminium alloy Al 1120 friction stir welds. Journal of Adhesion Science and Technology. 2020; 34(18): 2000–2010.
19. Wang W., Shi Q.Y., Liu P., Li H.K., Li T. A novel way to produce bulk SiCp reinforced aluminum metal matrix composites by friction stir processing. Journal of materials processing technology. 2009; 209(4): 2099–2103.
20. Mahmoud E.R., Ikeuchi K., Takahashi M. Fabrication of SiC particle reinforced composite on aluminium surface by friction stir processing. Science and technology of welding and joining. 2008; 13(7): 607–618.
21. Mishra R.S., Ma Z.Y., Charit I. Friction stir processing: a novel technique for fabrication of surface composite. Materials Science and Engineering: A. 2003; 341(1–2): 307–310.
22. Khodabakhshi F., Nosko M., Gerlich A.P. Effects of graphene nano-platelets (GNPs) on the microstructural characteristics and textural development of an Al-Mg alloy during friction-stir processing. Surface and Coatings Technology. 2018; 335: 288–305.
23. Deore H.A., Mishra J., Rao A.G., Mehtani H., Hiwarkar V.D. Effect of filler material and post process ageing treatment on microstructure, mechanical properties and wear behaviour of friction stir processed AA 7075 surface composites. Surface and Coatings Technology. 2019; 374: 52–64.
24. Tonelli L., Morri A., Toschi S., Shaaban M., Ammar H.R., Ahmed M.M., Ramadan R.M., El-Mahallawi I., Ceschini L. Effect of FSP parameters and tool geometry on microstructure, hardness, and wear properties of AA7075 with and without reinforcing B 4 C ceramic particles. The International Journal of Advanced Manufacturing Technology. 2019; 102: 3945–3961.
25. Rana, H., Badheka, V. Elucidation of the role of rotation speed and stirring direction on AA 7075-B4C surface composites formulated by friction stir processing. Proceedings of the Institution of Mechanical Engineers, Part L: Journal of Materials: Design and Applications. 2019; 233(5): 977–994. https://doi.org/10.1177/1464420717736548.
26. Hosseinzadeh, Ali, Amin Radi, and Guney Guven Yapici. Advanced Surface Enhancement of a High Strength Aluminum Alloy Through Friction Stir Processing. Proceedings of the 2nd International Conference on Advanced Surface Enhancement (INCASE 2021) Innovation Leading to Industrialization. Singapore: Springer Singapore, 2021. https://doi.org/10.1007/978–981–16–5763–4_2.
27. Butola, Ravi, et al. Mechanical and wear performance of Al/SiC surface composite prepared through friction stir processing. Materials Research Express 8.1. 2021; 016520. https:// doi.org/10.1088/2053–1591/abd89d
28. Martin A., Martinez M.A., Llorca J. Wear of SiC-reinforced Al-matrix composites in the temperature range 20–200 C. Wear. 1996; 193(2): 169–179.
29. Faisal N., Kumar K. Mechanical and tribological behaviour of nano scaled silicon carbide reinforced aluminium composites. Journal of Experimental Nanoscience. 2018; 13(sup1): S1–S3.
30. Kumar K.S., Kailas S.V. The role of friction stir welding tool on material flow and weld formation. Materials Science and Engineering: A. 2008; 485(1–2): 367–374.
31. Zhao, Yong, et al. Effect of friction stir processing with B 4 C particles on the microstructure and mechanical properties of 6061 aluminum alloy. The international journal of advanced manufacturing technology. 2015; (78): 1437–1443. https://doi.org/10.1007/s00170–014–6748–9
32. Aruri D., Adepu K., Adepu K., Bazavada K. Wear and mechanical properties of 6061-T6 aluminum alloy surface hybrid composites [(SiC+ Gr) and (SiC+ Al2O3)] fabricated by friction stir processing. journal of materials research and technology.

2013; 2(4): 362–369.

33. Huang G., Hou W., Li J., Shen Y. Development of surface composite based on Al-Cu system by friction stir processing: Evaluation of microstructure, formation mechanism and wear behavior. Surface and Coatings Technology. 2018; (344): 30–42.
34. Qu J., Xu H., Feng Z., Frederick D.A., An L., Heinrich H. Improving the tribological characteristics of aluminum 6061 alloy by surface compositing with sub-micro-size ceramic particles via friction stir processing. Wear. 2011; 271(9–10): 1940–1945.
35. Dinaharan, I. Influence of ceramic particulate type on microstructure and tensile strength of aluminum matrix composites produced using friction stir processing. Journal of Asian Ceramic Societies. 2016; 209–218.
36. Huang G., Hou W., Shen Y. Evaluation of the microstructure and mechanical properties of WC particle reinforced aluminum matrix composites fabricated by friction stir processing. Materials characterization. 2018; 138: 26–37.
37. Selvakumar S., Dinaharan I., Palanivel R., Babu B.G. Characterization of molybdenum particles reinforced Al6082 aluminum matrix composites with improved ductility produced using friction stir processing. Materials Characterization. 2017; 125: 13–22.
38. Lin Y., Zhang Y., Xiong B., Lavernia E.J. Achieving high tensile elongation in an ultra-fine grained Al alloy via low dislocation density. Materials Letters. 2012; 82: 233–236.
39. Ansari A.J., Anas M. Microstructure and Mechanical Behaviour of Reinforced Aluminium-Based Surface Composites Synthesized by Friction Stir Processing Route: A Review. Tailored Functional Materials: Select Proceedings of MMETFP 2021. 2022; (16): 397–408.